Associated $W^{\pm}H^{\mp}$ production at $e^{+}e^{-}$ and hadron colliders *

Oliver Brein
Max-Planck-Institut für Physik, München
E-mail: obr@mppmu.mpg.de

Abstract

We show some results in the minimal supersymmetric Standard Model (MSSM) and the two Higgs doublet model (THDM) for $W^{\pm}H^{\mp}$ production cross sections at $e^{+}e^{-}$ and hadron colliders. [1] We demonstrate that the predictions for the cross sections in the two models can be vastly different. Observing these processes, once the existence of a charged Higgs is established, might shed some light on the underlying model for an extended Higgs sector.

1 Introduction

Charged Higgs search and beyond:
The discovery of a charged Higgs boson at future colliders would be an unambiguous sign of an extended Higgs sector. The production of charged Higgs bosons at the Tevatron and the LHC will happen mainly via the partonic processes: $gb \to tH^{+}$ and $gg \to tbH^{+}$ [1]. Other partonic processes like charged Higgs pair production ($gg/q\bar{q} \to H^{+}H^{-}$) [2] and associated $W^{\pm}H^{\mp}$ production ($gg/b\bar{b} \to H^{\pm}W^{\mp}$) [5, 6, 7] have also been considered, but they lead to a much smaller rate at these colliders. At an $e^{+}e^{-}$ collider the main production process for charged Higgs bosons is pair production ($e^{+}e^{-} \to H^{+}H^{-}$) which is mediated mainly via Photon- and Z- exchange in the s-channel. If the collider energy is not sufficient for pair production (i.e. $\sqrt{s} < 2m_{H^{\pm}}$) the associated $W^{\pm}H^{\mp}$ production becomes dominant for $\sqrt{s} > m_W + m_{H^{\pm}}$. In this case the signal rate is much smaller because the process is effectively loop-induced.

The methods to discover the charged Higgs boson at the LHC seem to be well established by now [3]. Once it is found, one would like to learn more about the charged Higgs boson beyond its mere existence and its mass. But, the main production processes at LHC are rather insensitive to the underlying model. More interesting in this respect is the associated $W^{\pm}H^{\mp}$ production process. At an $e^{+}e^{-}$ collider the process is effectively loop-induced and at hadron colliders the gluon-fusion process is loop-induced. Loop-induced processes depend already at leading order on the virtual particles in the loops. Thus, with a cross section measurement of such a process one would gain information about the underlying model.

*Talk presented at the "10th International Conference on Supersymmetry and Unification of Fundamental Interactions, SUSY 02", DESY Hamburg, June 17-23 2002

[1] The Fortran codes to calculate the cross section predictions of the processes discussed here are available upon request.

MSSM parameter scenario:
We are interested in scenarios which potentially show large effects from virtual squarks and especially from Stops. Therefore, the MSSM parameter scenario used for the numerical results presented here has a rather low Squark mass scale and shows large mixing in the Stop sector. We choose: a) the common sfermion mass scale $M_{\mathrm{SUSY}} = 350\,\mathrm{GeV}$, b) the Stop mixing parameter $X_t = A_t - \mu \cot\beta = -800\,\mathrm{GeV}$, c) the supersymmetric Higgs mass parameter $\mu = 300\,\mathrm{GeV}$, d) the gaugino mass parameters $\approx \mathcal{O}(1\,\mathrm{TeV})$.

The main features of the resulting scenario are the following. a) No mass bounds from direct search results are violated and indirect constraints on the parameters coming from requiring vacuum stability and from experimental bounds on the electroweak precision observables are also fulfilled. b) The mass of the light Stop is of order $100\,\mathrm{GeV}$ and there is a large mass splitting between the two Stop mass eigenstates. c) The Stop mixing angle is approximately $45°$. Thus maximal mixing occurs, i.e. all entries in the Stop mixing matrix have approximately the same magnitude. d) The mass of the lightest MSSM Higgs boson m_h is almost maximal with respect to X_t (because $|X_t| \approx 2M_{\mathrm{SUSY}}$ [4]). Note that this scenario allows for the production of Stop pairs at the energy scales considered in the following sections and the decay of the charged Higgs into Stop and Sbottom will be kinematically allowed for $m_{H^\pm} \gtrsim 450\,\mathrm{GeV}$.

2 $W^\pm H^\mp$ production at the LHC

There are two partonic processes contributing to $W^\pm H^\mp$ production at hadron colliders like the LHC [2]. On the one hand there is the tree-level process $b\bar{b}$ annihilation and on the other hand there is the loop-induced gluon fusion process (see Figure 1). Both processes have been considered already in [5], but in the MSSM calculation squark loops had been neglected. The full MSSM prediction for the gluon-fusion process appeared much later [6, 7].

$b\bar{b}$ annihilation has to be considered if the bottom quark is treated as an active flavour in the proton. In Figure 1 all Feynman diagrams contributing on tree-level to the amplitude are displayed. There are s-channel exchange diagrams for each of the neutral Higgs bosons and a t-channel diagram including a virtual top quark. Recently, the QCD corrections to the $b\bar{b}$ annihilation process became known [9].

The gluon fusion process is mediated by loops of virtual quarks and squarks (see Figure 1). Thus, the amplitude naturally splits into two subsets, one consisting of the diagrams with quark loops (THDM amplitude) and the other consisting of all diagrams with squark loops (squark amplitude). Figure 1 shows essentially all types of Feynman diagrams that contribute to the process in the MSSM.

The reason why we treat a tree-level and a loop-induced process on equal footing is the much larger number of gluon fusion events compared to $b\bar{b}$ annihilation events at a high energy proton collider. Formally, the distributions of bottom quarks and anti-quarks are suppressed by one power of α_S compared to the gluon distribution which is of order one. This is because the bottom is a heavy quark which doesn't have a valence distribution in the proton. Therefore, its distribution is generated mainly by gluon splitting processes. By naively using the bottom quark distribution in order to estimate the hadronic cross section via $b\bar{b}$ annihilation it is well known that one overestimates the true cross section [8]. The

[2]The work presented in this section has been done in collaboration with Wolfgang Hollik and Shinya Kanemura [6].

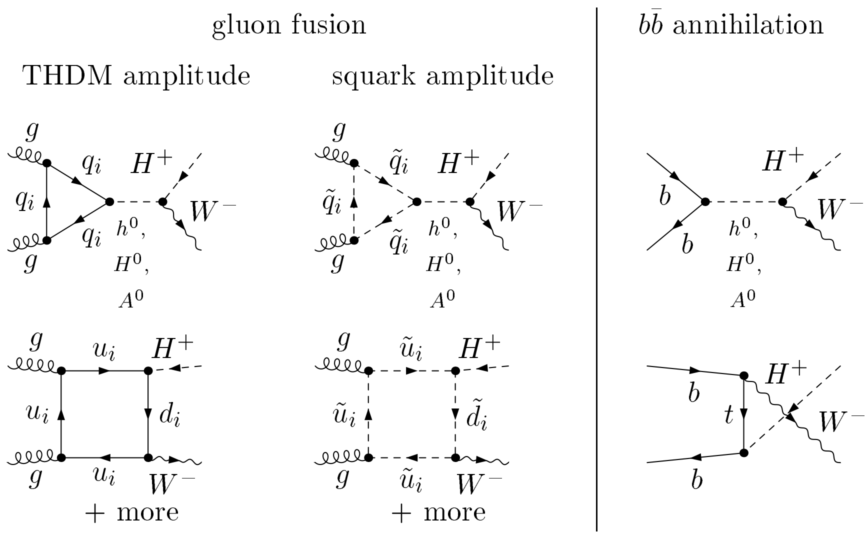

Figure 1: Typical Feynman diagrams for the partonic processes gluon fusion and $b\bar{b}$ annihilation contributing to $W^{\pm}H^{\mp}$ production at a hadron collider.

way to improve the prediction is to include additional processes of the same order in α_S like $gb \to bH^+W^-$ + c.c. or $gg \to b\bar{b}H^{\pm}W^{\mp}$. But then a suitable subtraction of configurations with collinear bottom quarks of these additional processes has to be applied in order to avoid double-counting contributions which are already resummed in the bottom quark distribution [3, 10]. In our analysis we use for the $b\bar{b}$ process the LO cross section with a running bottom mass instead of the pole mass as an approximation to the NLO result [9] which leads to a considerable reduction of the hadronic cross section. But still, this might be an overestimation.

MSSM results:

Naturally, the $b\bar{b}$ cross section is rather insensitive to the superpartner spectrum as no SUSY contributions appear at LO. The gluon fusion process shows, as expected, large sensitivity to the squark spectrum which appears in the loops. Especially, the squark contribution to the amplitude can get large due to threshold effects in the box loops. A striking feature of the quark loop contribution to the gluon fusion amplitude, already noted in [5], is a large destructive interference between quark loops of box- and triangle-type. Both partonic processes, $b\bar{b}$ annihilation and gluon fusion, are rather sensitive to the neutral Higgs sector. As a consequence, in the THDM the choice of the masses of the neutral Higgs bosons can influence the cross section dramatically (see section 2), whereas in the MSSM the neutral Higgs boson masses are essentially fixed, once values have been assigned to $m_{H^\pm}$ and $\tan\beta$.

Figure 2 shows the MSSM prediction for the hadronic cross section for $W^{\pm}H^{\mp}$ production at the LHC. The contributions from $b\bar{b}$ annihilation and gluon fusion are displayed separately as a function of the charged Higgs mass $m_{H^\pm}$ and $\tan\beta$. The results of the full MSSM (using the parameter scenario described above) are compared to a MSSM-like THDM (denoted by sTHDM in Figure 2). For the $b\bar{b}$ annihilation only one line, valid for both cases, is shown. The gluon fusion process instead is significantly different in the full MSSM and the MSSM-like THDM. The cross section via gluon fusion in the full MSSM can be up to an order of magnitude larger than in the sTHDM in our scenario. This is mainly due to threshold effects in the box-type squark loops which are not present in the sTHDM amplitude. The effect is maximal, if the production threshold ($m_W + m_{H^\pm}$) is somewhat below the position in $\sqrt{\hat{s}}$ ($= 2m_{\tilde{b}_1}$ (here $\approx 680\,\text{GeV}$)) where the threshold peak in the partonic cross section appears. This happens in the left plot in Figure 2 for $m_{H^\pm} \approx 450\,\text{GeV}$. For this interesting value of $m_{H^\pm}$ the right plot in Figure 2 shows the $\tan\beta$-dependence. One can see that the pronounced minimum in the MSSM-like THDM has completely disappeared in the full MSSM and especially for $\tan\beta$ up to about 15 the cross section for the gluon fusion process has the same order of magnitude as for the $b\bar{b}$ annihilation process. Of course for large $\tan\beta$ the $b\bar{b}$ annihilation process dominates.

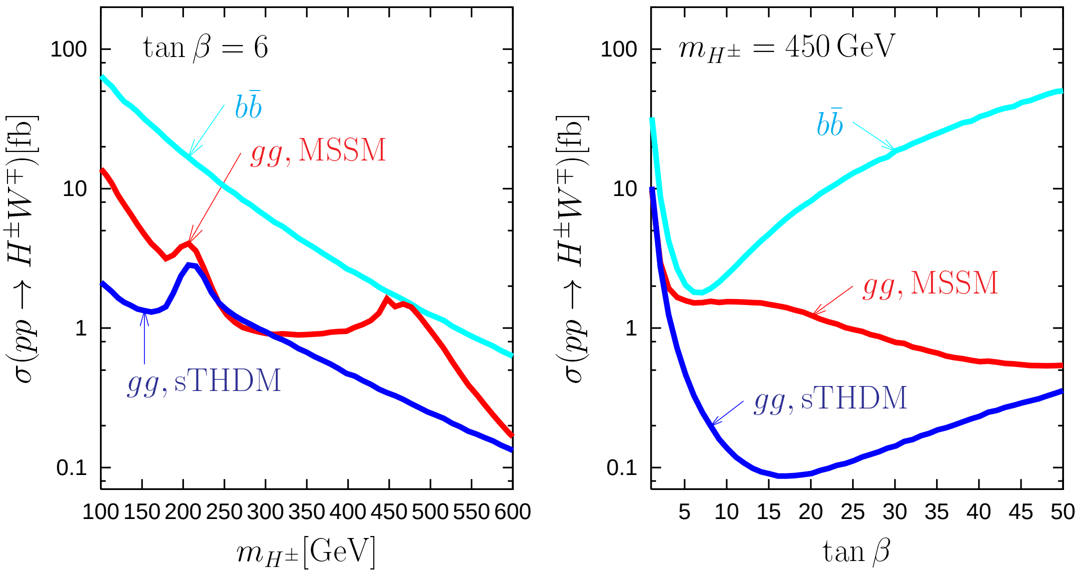

Figure 2: Hadronic cross section for $W^\pm H^\mp$ production via $b\bar{b}$ annihilation and gluon fusion as a function of $m_{H^\pm}$ and $\tan\beta$.

THDM results:

In the MSSM the mass relations among the Higgs bosons for large $m_{H^\pm}$ lead to

$$m_{h^0} = \mathcal{O}(100\text{GeV}),\ m_{H^0} \approx m_{A^0} \approx m_{H^\pm}\ .$$

This has some interesting consequences for the process under study. a) The contributions of neutral Higgs s-channel exchange cannot decouple from the process, because the masses of the heavy Higgs bosons are nearly degenerate. b) Resonant s-channel Higgs exchange is impossible in the MSSM, because the threshold $m_{H^\pm} + m_W$ is always larger than any of the masses of the neutral Higgs bosons (m_{h^0,H^0,A^0}). c) Therefore, the negative interference between box- and triangle-type quark loops in the gluon fusion amplitude seems to be unavoidable in the MSSM.

But this is not true in the general THDM. As all Higgs masses are free parameters, there can be resonant s-channel exchange of neutral Higgs bosons. It is also possible to choose some of the neutral Higgs bosons much heavier than the threshold ($m_{H^\pm} + m_W$), thus suppressing their contribution to the amplitude. Thus, in the general THDM the above-mentioned strong negative interference need not be present and therefore the cross section can be much larger than in the MSSM.

In Figure 3 one example for the typical behaviour in the general THDM is shown. We take $m_{H^\pm} = 400\,\mathrm{GeV}$, $\tan\beta = 6$ and the MSSM values for the mass of the lightest Higgs m_{h^0} and the mixing angle in the Higgs sector α. Figure 3 shows a contour plot of the hadronic cross section for $W^\pm H^\mp$ production via gluon fusion as a function of the neutral Higgs masses m_{A^0} and m_{H^0}. The point where the scenario coincides with a MSSM-like THDM is marked by a red cross (labelled sTHDM). In this case the cross section via gluon fusion is 0.48 fb (via $b\bar{b}$ annihilation: 2.7 fb). The parameter region displayed in Figure 3 is roughly the region which is compatible with negative direct search results for H^0 and A^0 bosons and the requirement of tree-level unitarity. Within the star-shaped region, bounded by the thick lines in the plot, the scenarios are compatible with the measured value of the electroweak rho-parameter. The cross section shows a steep rise if one of the Higgs masses, m_{A^0} or m_{H^0}, gets bigger than the $W^\pm H^\mp$ production threshold which is due to the resonant behavior of the corresponding s-channel exchange diagrams. But, even without any resonance in the partonic cross section near the $W^\pm H^\mp$ threshold the cross section can be up to a factor 500 larger than in the corresponding MSSM-like THDM (e.g. for $m_{A^0} = 800\,\mathrm{GeV}$ and $m_{H^0} = 400\,\mathrm{GeV}$ we have $\sigma = 470\,\mathrm{fb}$ via gluon fusion plus 860 fb via $b\bar{b}$ annihilation). It seems that some scenarios in the general THDM can be already distinguished from the MSSM just by looking at the rate of $W^\pm H^\mp$ production.

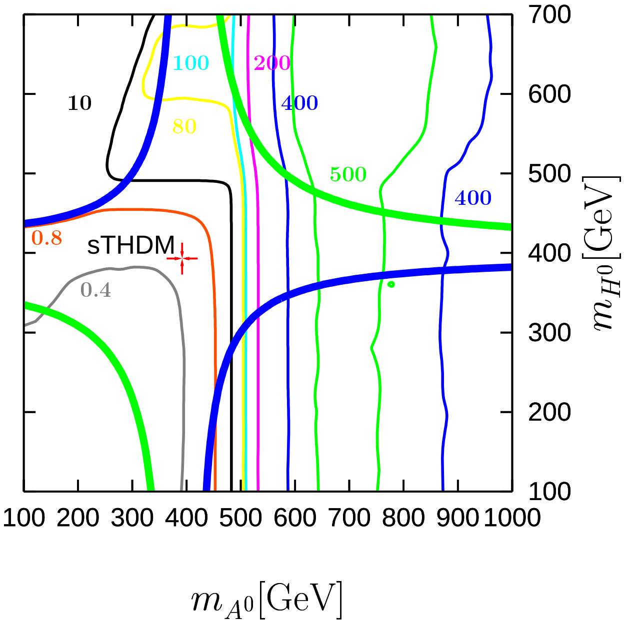

Figure 3: Hadronic cross section for $W^\pm H^\mp$ production via gluon fusion in fb as a function of the neutral Higgs masses m_{A^0} and m_{H^0} in the general THDM. The thin coloured lines represent lines of equal cross section. The parameter regions between the thick lines and the corners of the plot are excluded (see text).

3 $e^+e^- \to W^\pm H^\mp$

The leading contributions to the amplitude are one-loop Feynman diagrams (see Figure 4) [3]. There are diagrams with H–W and G–H mixing self energy insertions and there are triangle- and box-type diagrams which contain either only THDM particles or superpartners in the loop. The calculation of the cross section in the framework of the THDM has been done by several authors [11] and only recently the MSSM calculation has been done [12, 13].

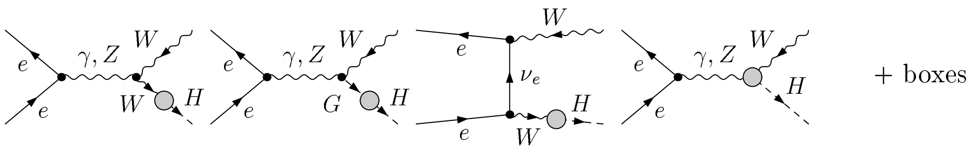

Figure 4: Feynman diagrams contributing to the amplitude of the process $e^+e^- \to W^+H^-$. Only generic one-loop vertex insertions are shown.

MSSM results:
Typically the vertex diagrams give the main contribution to the cross section. Especially, vertex graphs with loops of third generation quarks and squarks which couple to the outgoing charged Higgs boson are dominant. In Figure 5 the predicted cross section for the process $e^+e^- \to W^\mp H^\pm$ is displayed for the full MSSM using the scenario of section 1 and the corresponding MSSM-like THDM (sTHDM). The Figure shows examples for the $m_{H^\pm}$- and $\tan\beta$-dependence of the cross section. Generically, for large $\tan\beta$ the result for our MSSM scenario is considerably larger than for the corresponding THDM (up to two orders of magnitude), as exemplified by the $\tan\beta$-plot in Figure 5. The enhancement with respect to the sTHDM case is especially due to the squark-loop diagrams which contain enhanced couplings to the charged Higgs. The $m_{H^\pm}$-plot in Figure 5 shows the cross section for $\tan\beta = 30$, i.e. in the area of large enhancement with respect to $\tan\beta$. It is interesting that the MSSM prediction stays at least one order of magnitude larger than the sTHDM prediction over the entire charged Higgs mass range which is kinematically accessible.

The large differences between the MSSM prediction in our scenario and the corresponding THDM prediction suggest that, once a charged Higgs is found, one might gain valuable information about the underlying model it is embedded in by observing the associated production channel. The results presented here assume unpolarized beams. Note that optimal polarization of e^- and e^+ can increase the cross section almost by a factor of four. It seems that large corrections by neutralino and chargino loops are possible, but this issue is still under investigation [13].

4 Summary

We investigated the predictions of the MSSM and the THDM for $W^\pm H^\mp$ production at the LHC and a future high energy e^+e^- collider with 500 GeV center of mass energy. One interesting result for the hadron collider is that among the contributing partonic processes

[3] The work presented in this section has been done in collaboration with Thomas Hahn and Wolfgang Hollik [13].

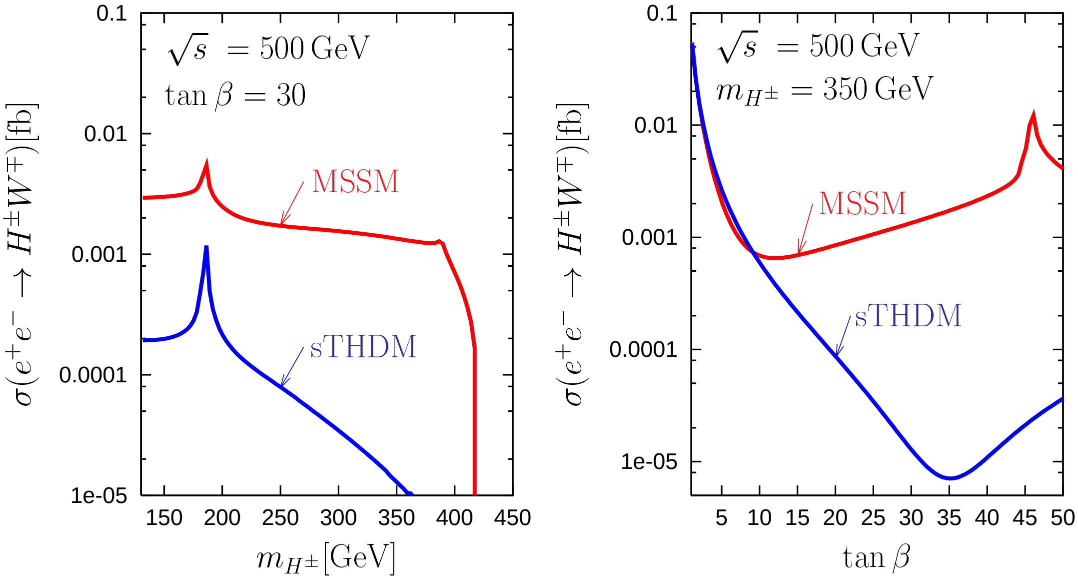

Figure 5: Unpolarized cross section for $e^+e^- \to H^\pm W^\mp$ for a center of mass energy of $\sqrt{s} = 500\,\text{GeV}$ as function of $m_{H^\pm}$ and $\tan\beta$. The predictions of the MSSM in our scenario and the corresponding MSSM-like THDM (sTHDM) are compared.

the loop-induced gluon-fusion can compete with the tree-level $b\bar{b}$ annihilation in certain cases. Therefore and with regard to the potential pitfall of overestimating the $b\bar{b}$ cross section, a careful treatment of the $b\bar{b}$ process is needed (see [9, 10]). Furthermore, we showed that the hadronic cross section in the general THDM can be much larger than in the MSSM (about a factor 500-1000). At a high energy e^+e^- collider the $W^\pm H^\mp$ production is especially important for the charged Higgs boson detection, if pair production is kinematically forbidden.

In general these loop-induced processes are highly model-dependent. Therefore, they are well suited to gain information about the underlying model. The MSSM scenarios with large Stop mixing and low sfermion mass scale, for which we showed here one example, can give rise to cross sections for $W^\pm H^\mp$ production at the LHC or e^+e^- machines which are significantly different from a MSSM-like THDM.

Acknowledgement

The results discussed here were obtained in collaboration with Shinya Kanemura, Wolfgang Hollik and Thomas Hahn. I thank the organizers of SUSY 2002 for creating a very pleasant meeting.

References

[1] Talk of T. Plehn, these proceedings; T. Plehn, hep-ph/0206121.

[2] E. Eichten *et al.*, Rev. Mod. Phys. **56** (1984) 579; N. G. Deshpande , X. Tata and D. A. Dicus, Phys. Rev. D **29** (1984) 1527; A. Krause *et al.*, Nucl. Phys. B **519** (1998) 85; A. A. Barrientos Bendezu and B. A. Kniehl, Nucl. Phys. B **568** (2000) 305; O. Brein and W. Hollik, Eur. Phys. J. C **13** (2000) 175.

[3] D. Cavalli *et al.*, hep-ph/0203056 and references therein.

[4] S. Heinemeyer, W. Hollik and G. Weiglein, Eur. Phys. J. C **9** (1999) 343.

[5] D. A. Dicus, J. L. Hewett, C. Kao and T. G. Rizzo, Phys. Rev. D **40** (1989) 787.

[6] O. Brein, W. Hollik and S. Kanemura, Phys. Rev. D **63** (2001) 095001.

[7] A. A. Barrientos Bendezu and B. A. Kniehl, Phys. Rev. D **59** (1999) 015009, Phys. Rev. D **63** (2001) 015009.

[8] F. I. Olness and W. K. Tung, Nucl. Phys. B **308** (1988) 813.

[9] Talk of S. h. Zhu, these proceedings; W. Hollik and S. h. Zhu, Phys. Rev. D **65** (2002) 075015.

[10] Talk of M. Spira, these proceedings;

[11] S. h. Zhu, hep-ph/9901221; S. Kanemura, Eur. Phys. J. C **17** (2000) 473; A. Arhrib, M. Capdequi Peyranere, W. Hollik and G. Moultaka, Nucl. Phys. B **581** (2000) 34.

[12] Talk of S. f. Su, these proceedings; H. E. Logan and S. f. Su, Phys. Rev. D **66** (2002) 035001.

[13] O. Brein, T. Hahn and W. Hollik, in preparation.